catalysts

MDPI

Review

Recent Advances in Synthesis and Applications of Carbon-Doped TiO_2 Nanomaterials

Li Hua [1], Zhengliang Yin [2] and Shunsheng Cao [2,*]

[1] Yangzhou Polytechnic Institute, College of Chemical Engineering, Yangzhou 225127, China; huali795@sohu.com

[2] Research School of Polymer Materials, School of Materials Science and Engineering, Jiangsu University, Zhenjiang 212013, China; ZhengLiangYin2020@126.com

* Correspondence: sscao@ujs.edu.cn; Tel.: +86-0511-88790191

Received: 26 October 2020; Accepted: 28 November 2020; Published: 8 December 2020

Abstract: TiO_2 has been widely used as a photocatalyst and an electrode material toward the photodegradation of organic pollutants and electrochemical applications, respectively. However, the properties of TiO_2 are not enough up to meet practical needs because of its intrinsic disadvantages such as a wide bandgap and low conductivity. Incorporation of carbon into the TiO_2 lattice is a promising tool to overcome these limitations because carbon has metal-like conductivity, high separation efficiency of photogenerated electron/hole pairs, and strong visible-light absorption. This review would describe and discuss a variety of strategies to develop carbon-doped TiO_2 with enhanced photoelectrochemical performances in environmental, energy, and catalytic fields. Emphasis is given to highlight current techniques and recent progress in C-doped TiO_2-based materials. Meanwhile, how to tackle the challenges we are currently facing is also discussed. This understanding will allow the process to continue to evolve and provide facile and feasible techniques for the design and development of carbon-doped TiO_2 materials.

Keywords: carbon doping; TiO_2; pollutant degradation; electrochemical application; review

1. Introduction

Environmental pollution and energy crisis have been the most urgent issues in recent years [1–5]. Photocatalysis is a promising strategy to alleviate, and even work out these problems because it could efficiently decompose organic pollutants or produce chemical energy using semiconductors and renewable solar energy [5–7]. Titanium dioxide (TiO_2), as one kind of nontoxic, high stable, and low-cost materials, has received special interest in environmental, catalysis, and energy areas [8–11]. However, the photocatalytic efficiency of pure TiO_2 is not enough up to meet practical needs because of its wide bandgap (~3.2 eV), and the fast recombination of photoinduced charge pairs, leading to a considerable energy consumption, poor visible-light photocatalytic activity, and low quantum efficiency [9,12,13]. Therefore, how to significantly promote charge separation is of significance in meeting practical needs.

Tremendous efforts have been devoted to varying the morphology, structure, and chemical composition of TiO_2 by doping metal and/or nonmetal elements, surface sensitization, and coupling with narrow band-gap semiconductors [8,12–14]. Among these strategies, metal doped TiO_2 usually suffers from photocorrosion, poor stability, low doping amount, and no noticeable change in the band gap of TiO_2 [8,14–16], while TiO_2 is coupled with other semiconductors, the additional cost and undermined stabilization have also disadvantageous effects on the practical employment of TiO_2 composites [15]. Notably, non-metal doping has attracted much more interest of investigators than metal doping in improving the photoelectronic performances of TiO_2 and in shifting its absorption edge to the long wavelength region [13,14]. Especially, carbon doped TiO_2 manifests promising

advantages beyond other non-metal doping, which may be ascribed to following aspects [12,14,17–20]: (1) carbon holds metallic conductivity; (2) carbon serves as a trapping center and transport channel for photogenerated electrons, promoting separation efficiency of photoinduced electron/hole pairs; and (3) carbon can also act as a sensitizer to sensitize TiO_2 under visible light irradiation, thus aggregating a number of thermal energy, facilitating charge transfer from the bulk of TiO_2 into oxidation reaction sites, and further generating lots of active species. Notably, carbon is always indicated that it can be permeated to the lattice of TiO_2 so as to substitute a lattice O or Ti atom, and then form a Ti–C or C–O–Ti bond, which produces a hybrid orbital just above the valence band of TiO_2 and bestows a significant enhancement in visible-light driven photocatalytic activity. Therefore, coupling TiO_2 with carbon materials including activated carbon [21,22], carbon nanofibers [23,24], carbon nanotubes [25–27], carbon sphere [28,29], carbon dot [30,31], graphene [32–34], and carbon doping [8,9,14,35] have been widely investigated and proved to hold significant potential over other types of modification methods in environmental, energy, and biomedical fields.

Among carbon materials, carbon doping has been attracting special interest because the introduction of carbon atom causes an electron coupling effect between carbon and TiO_2 or introduces a localized occupied state into TiO_2 to narrow the bandgap of TiO_2 [8,9,14]. For example, Zegeye et al. [36] developed hybrid carbon-doped TiO_2/S composite as a positive electrode material for lithium-sulfur batteries, manifesting enhanced cycle stability and rate performance. Our groups designed and constructed several carbon-doped TiO_2-based materials such as C-doped TiO_2 hollow spheres [14], C-doped TiO_2 single-crystal nanorods [8], and hierarchical SiO_2@C-doped TiO_2 hollow spheres [9]. Further investigation found that the as-synthesized carbon-doped TiO_2 materials manifested superior photocatalytic performance toward the degradation of organic pollutants (RhB-. MB, MV, 4-NP, etc.).

In the past several years, many encouraging achievements have been exhibited in the research area of TiO_2-based materials. Especially, carbon-doped TiO_2 composites have attracted an increasing attention in environmental and energy science because they can exhibit sizeable potential superiorities as adsorbent, support, and sensitizer, promoting photogenerated electrons migrating to semiconductors [7,37]. In this review, we systematically summarize the currently available synthesis strategies and applications of carbon-doped TiO_2 materials. Notably, we further highlight recent progress in the design and construction of carbon-doped TiO_2 composites with a multifunctional nature. Finally, challenges and outlooks are outlined and discussed, identifying prospective areas for related research in this field.

2. Characterization Techniques for the Formation of Carbon Doping

2.1. XPS Analysis

Carbon-doped TiO_2 is that carbon element is incorporated into the lattice of TiO_2 by replacing some of the lattice titanium or oxygen atoms, forming Ti−O–C or Ti−C bond, respectively. Therefore, X-ray photoelectron spectroscopy (XPS) measurement was widely used to obtain the information of Ti−O–C or Ti−C bond because XPS has a perfect match of its probe length (about 10 nm) to the size of particles, and exhibits its ability to probe the chemical identity of the elements present [38]. Therefore, the binding energy of C1s according to XPS analysis is considered as a solid evidence to confirm the formation of carbon doping [8,9,14,39–42], as shown in Table 1. This section focuses on addressing and discussing the difference of two chemical bonds (Ti−O–C or Ti−C band) as an evidence to distinguish whether carbon is incorporated into the lattice of TiO_2, adsorbed on the surface, or the interstitial position of the TiO_2 lattice.

Table 1. The C1s peak and typical synthetic method of C-doped TiO_2 materials.

Catalyst	C1s Peak	Synthesis Methods	Reference
Carbon@TiO_2 hollow spheres	Ti–O–C bond	Template-derected method	[12]
Carbon-TiO_2 nanotubes	Ti–O–C bond	Template-derected method	[13]
Carbon-doped TiO_2 on TiC structure	Ti–O–C bond	TiC calcination	[15]
C-doped TiO_2	Ti–O–C bond	Sol-microwave	[43]
Carbon-Doped TiO_2 /MCF-F	Ti–O–C bond	Hydrothermal synthesis	[5]
TiO_2/NCQD composites	Ti–O–C bond	TiC calcination	[44]
Fe_3O_4@C@F-TiO_2	Ti–O–C bond	Hydrothermal synthesis	[45]
Pd/TiO_2-C	Ti–O–C bond	Solvothermal synthesis	[46]
C-doped TiO_2 nanoparticles	Ti–C bond	Hydrothermal synthesis	[47]
C-doped TiO_2@g-C_3N_4 nanospheres	Ti–C bond	Hydrothermal synthesis	[48]
C-TiO_2 modified g-C_3N_4	Ti–C bond	TiC calcination	[49]
MC-Meso C-doped TiO_2/S	Ti–C bond	Hydrothermal synthesis	[36]
N & C doped TiO_2 supported Pt	Ti–C bond	Hydrothermal synthesis	[50]
C-TiO_2/g-C_3N_4 composite	Ti–C bond	TiC calcination	[51]
C–H–TiO_2	Ti–C bond	TiC calcination	[40]
Carbon-doped TiO_2 nanorods	Ti–C bond	Template-directed method	[8]
SiO_2@C-doped TiO_2 hollow spheres	Ti–C bond	Template-directed method	[9]
C-doped Hollow TiO_2	Ti–C bond	Template-directed method	[14]
C-doped porous TiO_2	Ti–C bond	Template-directed method	[42]

2.1.1. The Existence of Ti–O–C Bond

XPS measurement was usually employed to obtain the chemical state and binding energy of carbon-doped or carbon-decorated TiO_2 composites, ascertaining fundamental information on the interaction between C dopant and TiO_2 [5,8,35,40,41,48,50–53]. When carbon is doped into the TiO_2 lattice by replacing the lattice titanium, the Ti–O–C bond can be observed in the C1s spectra, as shown in Figure 1. Therefore, many investigators believe that the existence of the Ti–O–C bond can be effective evidence for ascertaining carbon doping in their as-synthesized TiO_2-based materials [16,36,37]. For example, Qi et al. [5] prepared carbon-doped TiO_2/MCF-F composite according to the observation of Ti−O−C bonds in XPS spectra of C1s. Li et al. [54] reported a novel method for the preparation of carbon-doped TiO_2 composites according to the formation of the Ti−O−C bond located at 288.4 eV. Similarly, S. Ivanov and coworkers [55] insisted that the existence of the Ti−O−C structure could be used as evidence for confirming the formation of C-doped TiO_2. However, the existence of the Ti−O−C bond is not completely ascribed to the existence of carbon doping. In most cases, surface and/or interstitial amorphous carbonate dopants in the TiO_2 lattice also result in the formation of Ti–O–C [15,40,41] because carboxyl or oxygen-containing carbon in GO sheets exhibits strong covalent binding ability to TiO_2 [12,41,56], narrowing band-gap energy and prompting its visible light absorption. Accordingly, the existence of the Ti–O–C bond is not solid evidence for ascertaining carbon incorporated into TiO_2 lattice, but it might be considered as a result of specifically interstitial carbon doping. Undoubtedly, more convincing evidence is required for confirming the formation of carbon doping in the TiO_2 lattice [39,53].

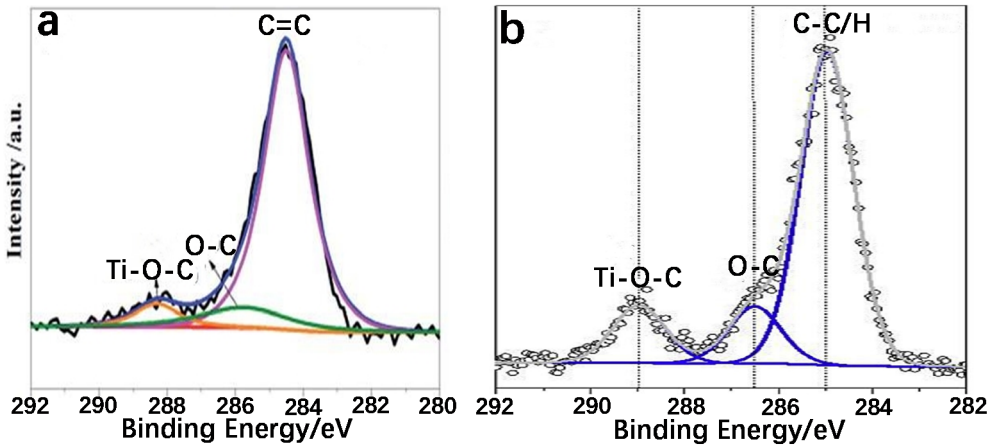

Figure 1. The existence of the Ti–O–C bond in XPS spectra of C1s (**a**) [54] and (**b**) [55].

2.1.2. The Existence of Ti–C Bond

When carbon is doped into the TiO_2 lattice by replacing lattice oxygen, Ti–C bond can be seen in the XPS spectra of C1s, as shown in Figure 2. it has been proved that the appearance of the Ti–C bond is considered as a solid evidence for confirming the formation of carbon doping in TiO_2-based materials [35,36,50]. For example, Dhanasekaran P. and coworkers ascertained the formation of carbon doped titanium oxide according to the peak at 282.7 eV (Ti–C bond) [50]. Recently, Wang et al. [35] successfully constructed carbon-doped TiO_2 nanotubes by referring the binding energy of 282.0 eV in the XPS spectra of C1s. Unlike Ti–O–C bond, the existence of Ti−C is the only result of carbon replacing oxygen in the TiO_2 lattice. Clearly, the existence of the Ti–C bond can be used as the most direct evidence for identifying the formation of carbon doping, as introduced in our previous workers [8,9,14,42]. Similarly, the absence of the Ti−C bond is considered as carbon decorated TiO_2 other than carbon doped TiO_2, suggesting that carbon species do not substitute oxygen species and dope into the TiO_2 lattice as reported in many publications [7,12,16,18,57–60].

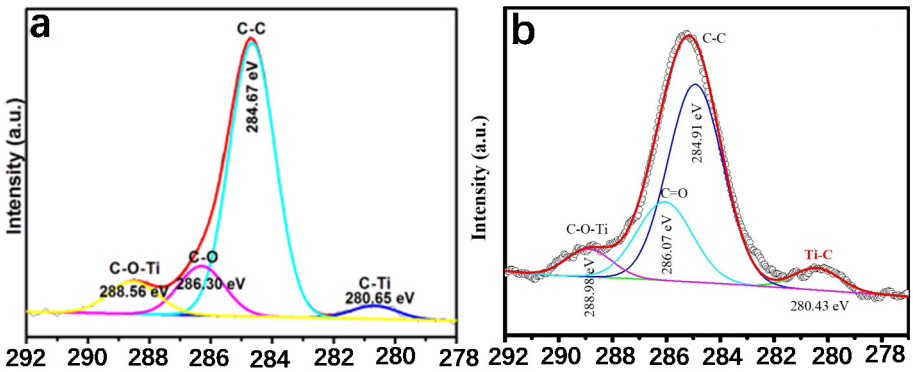

Figure 2. The existence of Ti–C bond in the XPS spectra of C1s (**a**) [14] and (**b**) [8].

2.2. EPR Analysis

Generally, electron paramagnetic resonance (EPR) analysis was widely used to evaluate the formation of defect sites in carbon or other dopants doped TiO_2-based materials because EPR can characterize the unpaired electrons or paramagnetic centers [40,61,62]. If carbon doping was formed in the TiO_2 lattice, a stronger EPR signatable 11 at $g = 2.003 \pm 0.001$ was more able to be observed than that of pure TiO_2 or undoped TiO_2, which could be ascribed to the unpaired electron trapped on surface oxygen vacancies, proving that carbon element could be incorporated into the crystal lattice of TiO_2-based materials [40,61].

3. Strategies for the Synthesis of C-Doped TiO_2 Materials

Various strategies including hydrothermal technique, template strategy, thermal oxidation of TiC, and sol–gel process have been introduced to construct carbon-doped TiO_2 materials with enhanced photoelectrochemical performances [16,17], as shown in Table 1. This section would pay attention to the description and discussion of synthetic methods involved in developing C-doped TiO_2-based materials.

3.1. Hydrothermal Method

As a simple and mature method, the hydrothermal technique has been widely used to construct C-doped TiO_2 materials because the morphology and structure of products are easily controlled by changing hydrothermal conditions [36,39,40,63]. In a typical hydrothermal synthesis, TiO_2 precursor and carbon source are dispersed or dissolved in acidic or alkaline solution, and then the mixture is transferred into a Teflon-lined autoclave, sealed, and heated in an electric oven (100–180 °C), forming crystallized C-TiO_2 structure. Finally, C-doped TiO_2 is successfully synthesized by removing organic residues via calcination under an air atmosphere. For example, mesoporous C-doped TiO_2 was able to be prepared via one-pot hydrothermal synthesis using $TiCl_4$ and sucrose as TiO_2 precursor and carbon source, respectively [36]. Aragaw et al. [53] introduced the preparation of Sn-C codoped single crystal TiO_2, in which $SnCl_4$ and glucose were used as tin and carbon dopant precursors, respectively. Qi D and coworkers reported C-doped TiO_2/MCF-F photocatalyst using silica mesoporous cellular foam (MCF) as host material and glucose as carbon source. Recently, our group in situ constructed C-doped TiO_2 single-crystal nanorod using CPS@TiO_2 as TiO_2 precursor and carbon dopant source [8], this preparation process and morphology are more clearly illustrated in Figure 3.

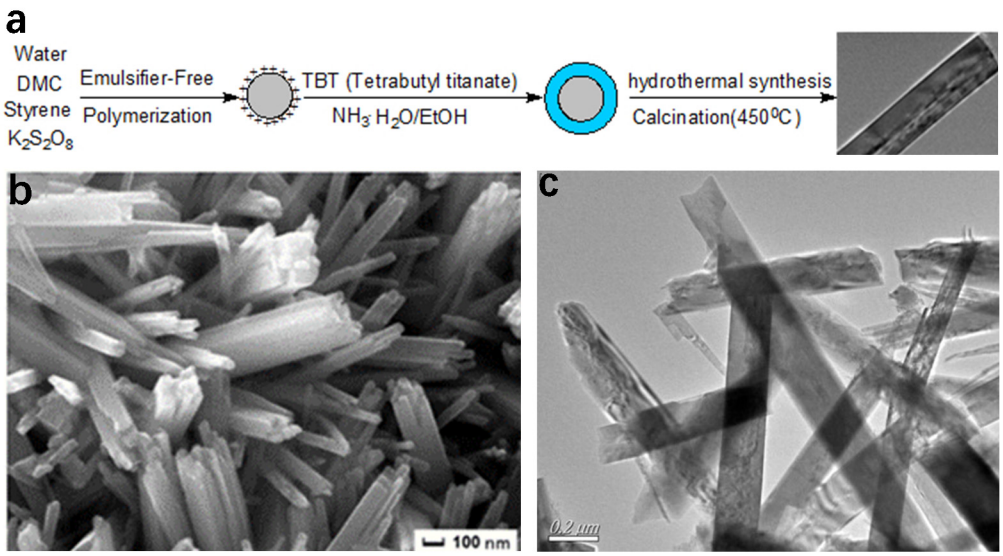

Figure 3. The demonstration (**a**), SEM (**b**), and TEM (**c**) of the C-TiO_2 single crystal nanorod. Reprinted with permission from Ref. [8].

In addition to being a one-pot and mature technique, hydrothermal method is advantageous in tuning the structure, morphology, and physical–chemical performances of final TiO_2 materials by changing TiO_2 precursor and hydrothermal conditions. Especially, hybrid functional TiO_2-based materials can be designed and constructed by adding other required species. Although the whole preparation process seems to be very simple, each step including the selection of the titanium dioxide precursor, hydrothermal condition, washing, and calcination presents a decisive role in tuning the morphology, structure, property, and yield of C-TiO_2 materials [63].

3.2. Template-Directed Method

Compared with solid/nonporous titanium dioxide nanoparticles, hollow/porous TiO_2 materials are more attractive because of a higher surface area and multiple interparticle scattering [14,64]. Precise control of the particle size, hollow/porous structure, and shell thickness of TiO_2 spheres has been a pursuing object because it is a key factor determining their properties [14]. In general, two main methods are introduced to prepare hollow TiO_2 spheres. One is template-free technique to construct hollow TiO_2 spheres via physical phenomenon [65]. Although the strategy can realize one-pot and large-scale production, a distinguished disadvantage is the concomitant production of TiO_2 spheres with an ill-shaped and fragile structure [13,14]. Another is the template-directed method that effectively tunes the shell and pore size of hollow TiO_2 spheres, overcoming the disadvantage of the template-free technique [14]. For example, Zou et al. [48] prepared C-doped hollow TiO_2 spheres using carbon sphere as a template. Matos and coworkers reported an easy and ecofriendly method to develop pristine anatase phase of C-doped TiO_2 using a biomass-derived molecule as a biotemplate [66]. Ji et al. [13] constructed C-doped TiO_2 nanotubes using surface-sulfonated polystyrene as a template through calcination. Our group introduced an in situ synthetic method for the development of hierarchical SiO_2@C-doped TiO_2 spheres with a uniform hollow structure using cationic polystyrene spheres as templates, as shown in Figure 4 [9], and then the facile strategy was further broadened to prepare various functionalized C-doped TiO_2 materials including C-doped hollow TiO_2 [14], C-doped porous TiO_2 [42], and C-doped TiO_2 single-crystal nanorods [8]. Although the template-directed method can develop various C-doped TiO_2 materials with a regular and tuned morphology at the nano- and/or microscale via controlling the structure of templates [63], its extensive applications may be limited because of the preparation cost and insufficient characterization of templates.

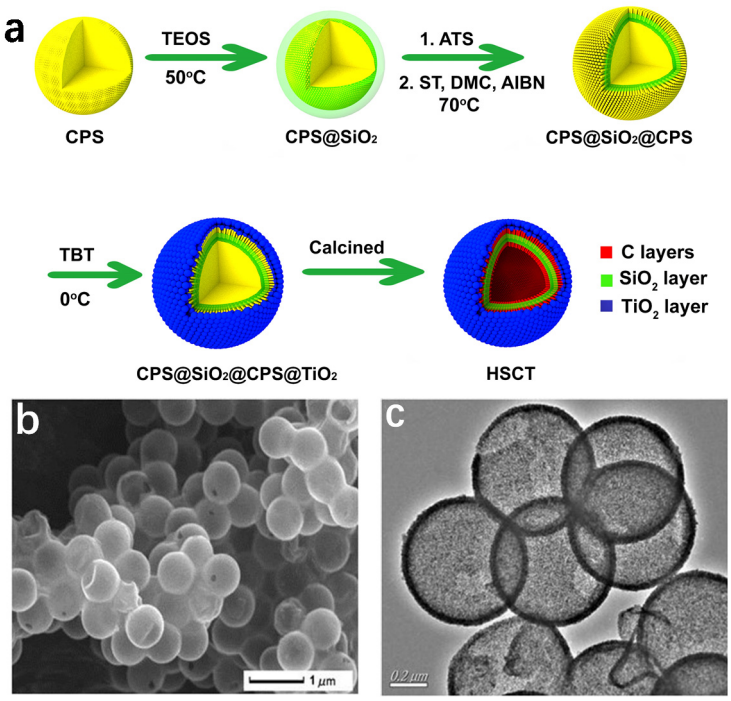

Figure 4. Preparation (**a**), SEM (**b**), and TEM (**c**) of the hierarchical SiO_2@C-doped TiO_2 spheres. Reprinted with permission from Ref. [9].

3.3. TiC Calcination

Titanium carbide (TiC) holds many fascinating properties including fast electron transfer, easy modification, and superior stabilization [15,44], making it more potential for the construction of C-doped TiO_2 materials via simple calcination because of its high visible-light absorption efficiency and

fast charge transfer. Yang et al. [15] prepared a C-doped layer on the TiC nanosphere with efficient visible light-photocatalytic H_2 production through in situ calcination of TiC. Figure 5 clearly demonstrated the preparation process, morphology, and structure of the as-synthesized porous C-doped TiO_2. Li et al. [54] reported C-doped TiO_2 multiple-phase composites exhibiting excellent ionic and electronic conductivity through the calcination of TiC at 600 °C for 10 h. Unfortunately, it is very difficult in preparing functionalized C-doped TiO_2 with controlled morphology, size, and hollow/porous structure via the calcination of TiC nanoparticle. Therefore, it is very necessary to combine other promising strategies for the development of C-doped TiO_2 materials with controllable structure and properties.

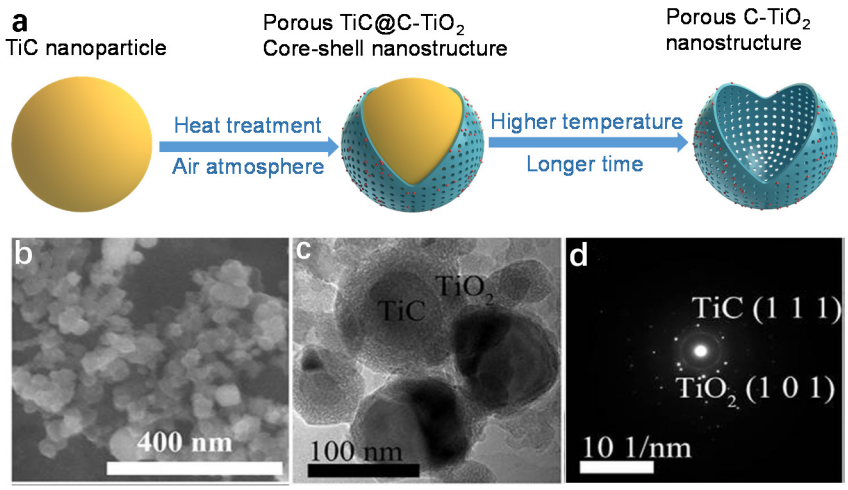

Figure 5. Preparation process (**a**), SEM (**b**), TEM (**c**), and SAED pattern (**d**) of porous C-TiO_2 nanostructure. Reprinted with permission from Ref. [15].

4. Application of C-Doped TiO_2 Materials

4.1. The Removal of Organic Pollutants

Exploiting effective strategies to remove organic pollutants in wastewater is very necessary according to environmental safety regulations due to increasing concerns about drinking water safety [67,68]. Photocatalysis has been considered as a promising way to remove organic contaminants including refractory organic pollutants by using solar energy because it can mineralize various organic pollutants to produce CO_2, H_2O, and other harmless small molecules. It is well known that pure TiO_2 holds poor visible-light absorption, low quantum yield, and undesired recombination of photogenerated charges. Notably, C-doped TiO_2 not only can effectively promote charge separation, but also can shift the optical response of TiO_2 from UV to visible spectral region, leading to an enhanced photocatalytic performance for the removal of various organic pollutants (Table 2) [8,9,39,69]. For example, Ji et al. [13] reported that C-doped TiO_2 nanotubes demonstrated much better photocatalytic activity toward the degradation of UDMH than bare TiO_2 under UV and visible light, as shown in Figure 6. Figure 6c demonstrated its photodegradation mechanism: under light irradiation, photogenerated electrons transferred more efficiently to conduction band of TiO_2 because carbon in the carbon-TiO_2 nanotubes could act as an electron trap, inhibiting charge recombination [70,71]. Furthermore, carbon also could improve adsorption of pollutant molecules, promoting photocatalytic performance because adsorption was normally the first step in photocatalysis [67,72].

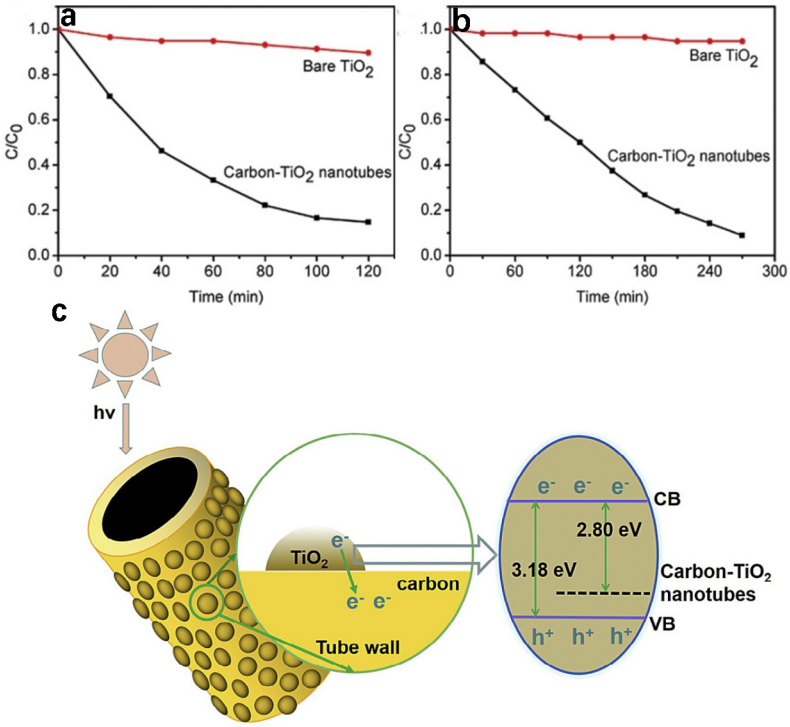

Figure 6. Photocatalytic degradation of UDMH solution by the carbon-TiO_2 nanotubes and bare TiO_2 under UV light (**a**), visible light (**b**), and photocatalytic mechanism (**c**). Reprinted with permission from Ref. [13].

Yu et al. [39] found that C-doped TiO_2 encapsulated with nano-sized graphene manifested superior visible-light performance for phenol degradation than those of anatase TiO_2, P25, and bare C-doped TiO_2. Zhang et al. [5] confirmed that C-doped TiO_2/MCFF exhibited good adsorptive ability and visible-light photocatalytic performance for degrading methyl orange. Our previous works also ascertained that C-doped TiO_2-based materials manifested stronger visible-light performances toward the removal of various contaminants including rhodamine B (RhB), methylene blue (MB), and p-nitrophenol [8,9,14]. The enhanced photocatalytic performance may be attributed to the synergistic effect between C-doping and TiO_2, in which carbon can generate electrons under visible light illumination, and then photoelectrons would be transferred to the contribution band of TiO_2, improving its efficient light harvesting and photocatalytic activity [17,73,74]. It is should be pointed out that the porous/hollow structure of photocatalysts is very beneficial to increase the surface area of photocatalyst and promote the contact probability of catalyst and substrate by decreasing diffusion limitation [9,14,75], which leads to better photocatalytic degradation of organic pollutants.

Table 2. The photocatalytic performance of C-doped TiO_2 materials toward the degradation of organic pollutants.

Catalyst	Pollutants	Degradation Rate	Enhanced Performance	Reference
Carbon-TiO_2 nanotubes	Unsymmetrical dimethylhydrazine	90%	10% for bare TiO_2	[13]
Mesoporous C-TiO_2	Methylthionine chloride	100%	Improve 10 times than P25	[75]
C-doped anatase TiO_2	Methylene blue	90%	3.7 times higher than TiO_2	[66]
C-doped ultra-small TiO_2	Toluene	85%	Less than 60% for bare $USTiO_2$	[76]
C-doped TiO_2/α-Fe_2O_3 heterojunction	Bisphenol A	79%	2.7 times higher than pristine TiO_2	[77]
C-doped TiO_2/anatase (A)/rutile (R)	Nonylphenol	41%	8% for undoped TiO_2	[78]
C/N-doped TiO_2	Microplastics (MPs)	71.77 ± 1.88%	Combined effect of pH and temperature driving the photodegradation of MPs	[79]
C-TiO_2	Rhodamine B	83.3% (75 min)	Around 15.0% higher than that of P-25	[80]
Carbon doping and coating of TiO_2	Methylene blue	85%	5 times higher than pristine TiO_2	[81]
Carbon-doped TiO_2	Caffeic Acid	92%	High adsorption and degradation	[82]
N/C co-doped TiO_2	Fluoroquinolone antibiotics (LEV)	95.7%	No visible light activity for Degussa P25	[83]
S, N and C doped mesoporous anatase brookite TiO_2	Microcystic toxins	100%	12.2% for un-doped TiO_2	[84]
TiO_2@C microspheres	Congo red	94%	2.7 times higher than N-TiO_2	[16]
Carbon-doped TiO_2 film	Methyl ethyl ketone	94%	41% for P25	[85]

4.2. Electrochemical Application

A variety of experiments have been proved that TiO_2 is a very promising electrode material for electrochemical applications due to its low cost, ideal capacitive response, and good cyclic stability [42,86–88], however, TiO_2 has many disadvantages including low conductivity, fast charge recombination, and high photochemical stability, leading to a poor electrochemical performance [48,55,89,90]. The introduction of carbon doping is a potential tool to efficiently improve the electrical conductivity of TiO_2-based materials because carbon holds good corrosion resistance, cyclic stability, and a long service lifetime during charge/discharge processes [58,86,87], as shown in Table 3. Shen et al. [86] found that hierarchical carbon-doped TiO_2 beads featured higher electronic conductivity than P25 and anatase TiO_2 beads. Our previous work also demonstrated that C-doped porous TiO_2 electrodes [42] increased ion diffusion channels and accelerated ion transfer, leading to an enhanced electrochemical performance, as shown in Figure 7. Notably, mesoporous/hollow electrode materials can exhibit high accessible area and ionic transport [11,36,42,58], resulting in enhanced electrochemical performances. Besides, the synergistic effect of multicomponent materials is of significance in promoting the electrochemical properties of carbon-doped TiO_2 [50,56,91,92].

Table 3. The photocatalytic performance of C-doped TiO_2 materials toward the degradation of organic pollutants.

Electrode Materials	Application Fields	Advantage	Comparative Performance	Stability	Reference
MC-Meso C-doped TiO_2/S	Lithium-sulfur batteries	802 mAh g^{-1}	530 mAh g^{-1} for mesoporous C-doped TiO_2/S	97.1% after 140 cycles	[36]
N&C doped TiO_2 supported Pt	Fuel cells	980 mW cm^{-2}	470 mW cm^{-2} for Pt/TiON-1	Durability test over 50,000 cycles	[50]
Si/TiO_2-CC composite	Lithium-ion battery	3.21 mAh cm^{-2}	More excellent areal capacity than other silicon composite anodes	Maintain 94.5% after 100 cycles	[92]
Carbon-Doped TiO_2-Bronze Nanowires	Lithium-ion Batteries	345 mAh g^{-1}	342 mAh g^{-1} for TB-NWs	Maintain 89% after 1000 cycles	[93]
TiO_2@C nanosheets	Na-ion batteries	264.9 mAh g^{-1}	170.8 mAh g^{-1} for pure carbon	After 100 cycles at 100 mA g^{-1}	[11]
S/C co-doped anatase	Lithium ion storage	210 mAh g^{-1}	Better electrochemical performance than non-doped TiO_2	83% capacity retention for 500 cycles	[56]
C-doped Hollow TiO_2	Supercapacitor	418 F g^{-1}	283 F g^{-1} for P25	78.1% capacity retention for 10,000 cycles	[94]
C-doped porous TiO_2	Supercapacitor	485 F g^{-1}	283 F g^{-1} for P25	~70% capacity retention for 1000 cycles	[42]

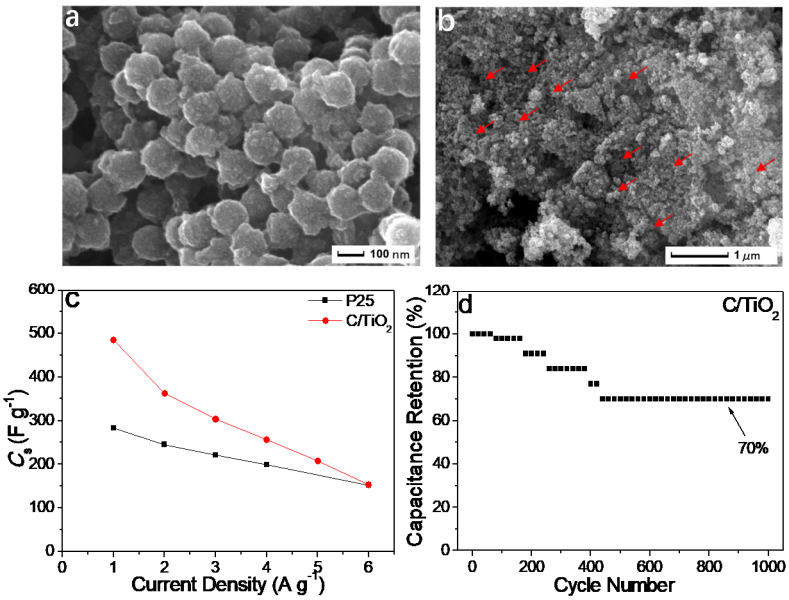

Figure 7. SEM (**a**,**b**) mages of C-doped porous TiO_2 electrodes, (**c**) comparative specific capacitances, and (**d**) cycling performance over 1000 cycles. Reprinted with permission from Ref. [42].

5. Summary and Outlook

Although carbon doping can efficiently enhance photoelectrochemical properties of TiO_2, it is still a very challenging task in obtaining a high doping amount of carbon in the TiO_2 lattice because C-doped TiO_2 is probably more difficult to be prepared than other non-mental doping [16], especially for

single crystal or single-crystal-like TiO_2 due to its high crystallinity [8,91], which hinders its further applications in environmental, energy, and catalytic fields. Co-doping with two or more dopants is a promising way to further enhance the properties of TiO_2 compared to their single doped or undoped TiO_2 counterparts due to a strong synergistic effect between these codopants within the TiO_2 matrix [53,95,96]. Zegeye et al. [36] reported that MC-Meso C-dopedTiO_2/S showed the best cycling stability and enhanced electrochemical property for lithium-sulfur batteries. Zhou et al. [7] found that In_2O_3 and carbon codoped TiO_2 could oxidize Hg^0 and manifested higher visible-light photoactivity compared with P25. Our previous works showed that C/N-TiO_2 hollow sphere [95] and C/Bi-TiO_2 single crystal nanorod [97] both exhibited an enhanced photocatalytic performance toward the removal of refractory organic pollutants. Unfortunately, it is extremely difficult in figuring out the contribution of carbon doping in codoped TiO_2-based materials. On the other hand, how to obtain uniform dispersion of carbon doping in the TiO_2 lattice also remains a big challenge [86]. Therefore, it is envisioned that future research will provide new insights in optimizing existing strategies and developing new techniques, which better construct C-doped TiO_2 materials with a high doping amount and controlled distribution of carbon.

Author Contributions: Conceptualization, L.H. and S.C.; data curation, S.C. and Z.Y.; original draft preparation, L.H.; writing—review and editing, S.C. and Z.Y.; supervision, S.C.; project administration, S.C. All authors have read and agreed to the published version of the manuscript.

Funding: The authors would like to thank the "Blue Project" in Jiangsu Colleges and Universities (2019-69) for financial supports to carry out this work.

Conflicts of Interest: The authors declare no conflict of interest.

References

1. Li, X.; Yu, J.; Jaroniec, M. Hierarchical photocatalysts. *Chem. Soc. Rev.* **2016**, *45*, 2603–2636. [CrossRef]
2. Liu, S.; Tang, Z.; Sun, Y.; Colmenares, J.C.; Xu, Y. One-dimension-based spatially ordered architectures for solar energy conversion. *Chem. Soc. Rev.* **2015**, *44*, 5053–5075. [CrossRef] [PubMed]
3. Zhao, S.; Chen, J.; Liu, Y.; Jiang, Y.; Jiang, C.; Yin, Z.; Xiao, Y.; Cao, S. Silver Nanoparticles Confined in Shell-in-Shell Hollow TiO_2 Manifesting Efficiently Photocatalytic Activity and Stability. *Chem. Eng. J.* **2019**, *367*, 249–259. [CrossRef]
4. Shi, Q.; Zhang, Y.; Sun, D.; Zhang, S.; Tang, T.; Zhang, X.; Cao, S. Bi2O3-Sensitized TiO2 Hollow Photocatalyst Drives the Efficient Removal of Tetracyclines under Visible Light. *Inorgan. Chem.* **2020**. [CrossRef]
5. Qi, D.; Xing, M.; Zhang, J. Hydrophobic Carbon-Doped TiO_2/MCF F Composite as a High Performance Photocatalyst. *J. Physical. Chem. C* **2014**, *118*, 7329–7336. [CrossRef]
6. Yin, Z.; Xie, L.; Cao, S.; Xiao, Y.; Chen, G.; Jiang, Y.; Wei, W.; Wu, L. Ag/Ag2O confined visible-light driven catalyst for highly efficient selective hydrogenation of nitroarenes in pure water medium at room temperature. *Chem. Eng. J.* **2020**, *394*, 125036. [CrossRef]
7. Zhou, X.; Wu, J.; Li, Q.; Zeng, T.; Ji, Z.; He, P.; Pan, W.; Qi, X.; Wang, C.; Liang, P. Carbon decorated In_2O_3/TiO_2 heterostructures with enhanced visible light-driven photocatalytic activity. *J. Catal.* **2017**, *355*, 26–39. [CrossRef]
8. Shao, J.; Sheng, W.; Wang, M.; Li, S.; Chen, J.; Zhang, Y.; Cao, S. In situ synthesis of carbon-doped TiO_2 single-crystal nanorods with a remarkably photocatalytic efficiency. *Appl. Catal. B Environ.* **2017**, *209*, 311–319. [CrossRef]
9. Zhang, Y.; Chen, J.; Hua, L.; Li, S.; Zhang, X.; Sheng, W.; Cao, S. High photocatalytic activity of hierarchical SiO_2@C-doped TiO_2 hollow sphere in UV and visible light towards degradation rhodamine B. *J. Hazard. Mater.* **2017**, *340*, 309–318. [CrossRef]
10. Guo, Q.; Zhou, C.; Ma, Z.; Ren, Z.; Fan, H.; Yang, X. Elementary photocatalytic chemistry on TiO_2 surfaces. *Chem. Soc. Rev.* **2016**, *45*, 3701–3730. [CrossRef]
11. Zhang, Q.; He, H.; Huang, X.; Yan, J.; Tang, Y.; Wang, H. TiO_2@C nanosheets with highly exposed (001) facets as a high-capacity anode for Na-ion batteries. *Chem. Eng. J.* **2018**, *332*, 57–65. [CrossRef]
12. Wang, W.; Xu, D.; Cheng, B.; Yu, J.; Jiang, C. Hybrid carbon@TiO_2 hollow spheres with enhanced photocatalytic CO_2 reduction activity. *J. Mater. Chem. A* **2017**, *5*, 5020–5029. [CrossRef]

13. Ji, L.; Zhang, Y.; Miao, S.; Gong, M.; Liu, X. In situ synthesis of carbon doped TiO_2 nanotubes with an enhanced photocatalytic performance under UV and visible light. *Carbon* **2017**, *125*, 544–550. [CrossRef]
14. Zhang, Y.; Zhao, Z.; Chen, J.; Cheng, L.; Chang, J.; Sheng, W.; Hu, C.; Cao, S. C-doped Hollow TiO_2 Spheres: In situ Synthesis, Controlled Shell Thickness, and Superior Visible-light Photocatalytic Activity. *Appl. Catal. B Environ.* **2015**, *165*, 715–722. [CrossRef]
15. Yang, C.; Zhang, X.; Qin, J.; Shen, X.; Yu, R.; Ma, M.; Liu, R. Porous carbon-doped TiO_2 on TiC nanostructures for enhanced photocatalytic hydrogen production under visible light. *J. Catal.* **2017**, *347*, 36–44. [CrossRef]
16. Guo, H.; Zheng, Z.; Chen, J.; Weng, W.; Huang, M. Facile template-free one-pot fabrication of TiO_2@C microspheres with high visible-light photocatalytic degradation activity. *J. Ind. Eng. Chem.* **2016**, *36*, 306–313. [CrossRef]
17. Liu, J.; Zhang, Q.; Yang, J.; Ma, H.; Tade, M.O.; Wang, S.; Liu, J. Facile synthesis of carbon-doped mesoporous anatase TiO_2 for the enhanced visible-light driven photocatalysis. *Chem. Commun.* **2014**, *50*, 13971–13974. [CrossRef]
18. Shao, Y.; Cao, C.; Chen, S.; He, M.; Fang, J.; Chen, J.; Li, X.; Li, D. Investigation of nitrogen doped and carbon species decorated TiO_2 with enhanced visible light photocatalytic activity by using chitosan. *Appl. Catal. B Environ.* **2015**, *179*, 344–351. [CrossRef]
19. Jia, J.; Li, D.; Wan, J.; Yu, X. Characterization and mechanism analysis of graphite/C-doped TiO_2 composite for enhanced photocatalytic performance. *J. Ind. Eng. Chem. Res.* **2016**, *33*, 162–169. [CrossRef]
20. Zhang, P.; Shao, C.; Zhang, Z.; Zhang, M.; Mu, J.; Guo, Z.; Liu, Y. TiO_2@carbon core/shell nanofibers: Controllable preparation and enhanced visible photocatalytic properties. *Nanoscale* **2011**, *3*, 2943–2949. [CrossRef]
21. Choi, H.; Kim, J.; Kim, H.; Lee, S.; Lee, Y. Improving the Electrochemical Performance of Hybrid Supercapacitor using Well-organized Urchin-like TiO_2 and Activated Carbon. *Electrochim. Acta* **2016**, *208*, 202–210. [CrossRef]
22. Ribeiro, E.; Plantard, G.; Teyssandier, F.; Maury, F.; Sadiki, N.; Chaumont, D.; Goetz, V. Activated-carbon/TiO_2 composites preparation: An original grafting by milling approach for solar water treatment applications. *J. Environ. Chem. Eng.* **2020**, *8*, 104115. [CrossRef]
23. Cao, N.; Gu, M.; Gao, M.; Li, C.; Liu, K.; Zhao, X.; Feng, J.; Ren, Y.; Wei, T. A three-layer photocatalyst carbon fibers/TiO_2 seed/TiO_2 nanorods with high photocatalytic degradation under visible light. *Appl. Surf. Sci.* **2020**, *530*, 147289. [CrossRef]
24. Huo, J.; Xue, Y.; Wang, X.; Liu, Y.; Zhang, L.; Guo, S. TiO_2/carbon nanofibers doped with phosphorus as anodes for hybrid Li-ion capacitors. *J. Power Source* **2020**, *473*, 228551. [CrossRef]
25. Naoi, K.; Kurita, T.; Abe, M.; Furuhashi, T.; Abe, Y.; Okazaki, K.; Miyamoto, J.; Iwama, E.; Aoyagi, S.; Naoi, W.; et al. Ultrafast Nanocrystalline-TiO_2(B)/Carbon Nanotube Hyperdispersion Prepared via Combined Ultracentrifugation and Hydrothermal Treatments for Hybrid Supercapacitors. *Adv. Mater.* **2016**, *28*, 6751–6757. [CrossRef] [PubMed]
26. Song, L.; Chen, P.; Li, Z.; Du, P.; Yang, Y.; Li, N.; Xiong, J. Flexible carbon nanotubes/TiO_2/C nanofibrous film as counter electrode of flexible quasi-solid dye-sensitized solar cells. *Thin Solid Films* **2020**, *711*, 138307. [CrossRef]
27. Basha, G.M.T.; Srikanth, A.; Venkateshwarlu, B. Effect of reinforcement of carbon nanotubes on air plasma sprayed conventional Al_2O_3-3%TiO_2 ceramic coatings. *Mater. Today Proceed* **2020**, *20*, 191–194. [CrossRef]
28. Wu, H.; Wu, X.; Wang, Z.; Aoki, H.; Kutsuna, S.; Jimura, K.; Hayashi, S. Anchoring titanium dioxide on carbon spheres for high-performance visible light photocatalysis. *Appl. Catal. B Environ.* **2017**, *207*, 255–266. [CrossRef]
29. Yao, J.; Mei, T.; Cui, Z.; Yu, Z.; Xu, K.; Wang, X. Hollow carbon spheres with TiO_2 encapsulated sulfur and polysulfides for long-cycle lithium-sulfur batteries. *Chem. Eng. J.* **2017**, *330*, 644–650. [CrossRef]
30. Cheng, C.; Tan, X.; Lu, D.; Wang, L.; Sen, T.; Lei, J.; El-Toni, A.M.; Zhang, J.; Zhang, F.; Zhao, D. Carbon-Dot-Sensitized, Nitrogen-Doped TiO_2 in Mesoporous Silica for Water Decontamination through Nonhydrophobic Enrichment-Degradation Mode. *Chem. Eng. J.* **2015**, *21*, 17944–17950.
31. Shahnazi, A.; Nabid, M.R.; Sedghi, R. Synthesis of surface molecularly imprinted poly-*o*-phenylenediamine/TiO_2/carbon nanodots with a highly enhanced selective photocatalytic degradation of pendimethalin herbicide under visible light. *React. Funct. Polym.* **2020**, *151*, 104580. [CrossRef]

32. Zhang, Y.; Foster, C.W.; Banks, C.E.; Shao, L.; Hou, H.; Zou, G.; Chen, J.; Huang, Z.; Ji, X. Graphene-Rich Wrapped Petal-Like Rutile TiO_2 tuned by Carbon Dots for High-Performance Sodium Storage. *Adv Mater.* **2016**, *28*, 9391–9399. [CrossRef] [PubMed]
33. Xu, C.; Kou, X.; Cao, B.; Fang, H. Hierarchical graphene@TiO_2 sponges for sodium-ion storage with high areal capacity and robust stability. *Electrochim. Acta* **2020**, *355*, 136782. [CrossRef]
34. Sadeghian, Z.; Hadidi, M.R.; Salehzadeh, D.; Nemati, A. Hydrophobic octadecylamine-functionalized graphene/TiO_2 hybrid coating for corrosion protection of copper bipolar plates in simulated proton exchange membrane fuel cell environment. *Int. J. Hydrogen Energ.* **2020**, *45*, 15380–15389. [CrossRef]
35. Wang, G.; Feng, H.; Hu, L.; Jin, W.; Hao, Q.; Gao, A.; Peng, X.; Li, W.; Wong, K.; Wang, H.; et al. An antibacterial platform based on capacitive carbon-doped TiO_2 nanotubes after direct or alternating current charging. *Nat. Commun.* **2018**, *9*, 2055. [CrossRef] [PubMed]
36. Zegeye, T.A.; Kuo, C.J.; Wotango, A.S.; Pan, C.; Chen, H.; Haregewoin, A.M.; Cheng, J.; Su, W.; Hwang, B. Hybrid nanostructured microporous carbon-mesoporous carbon doped titanium dioxide/sulfur composite positive electrode materials for rechargeable lithium-sulfur batteries. *J. Power Sources* **2016**, *32*, 239–252. [CrossRef]
37. Trevisan, V.; Olivo, A.; Pinna, F.; Signoretto, M.; Vindigni, F.; Cerrato, G.; Bianchi, C.L. C-N/TiO_2 photocatalysts: Effect of co-doping on the catalytic performance under visible light. *Appl. Catal. B Environ.* **2014**, *160*, 152–160. [CrossRef]
38. Cao, S.; Liu, B.; Deng, X.; Luo, R.; Chen, H. A novel approach for the preparation of acrylate–siloxane particles with core–shell structure. *Polym. Int.* **2006**, *56*, 357–363. [CrossRef]
39. Yu, S.; Yun, H.; Kim, Y.; Yi, J. Carbon-doped TiO_2 nanoparticles wrapped with nanographene as a high performance photocatalyst for phenol degradation under visible light irradiation. *Appl. Catal. B Environ.* **2014**, *144*, 893–899. [CrossRef]
40. Zeng, L.; Song, W.; Li, M.; Zeng, D.; Xie, C. Catalytic oxidation of formaldehyde on surface of H TiO_2/H C TiO_2 without light illumination at room temperature. *Appl. Catal. B Environ.* **2014**, *147*, 490–498. [CrossRef]
41. Liu, J.; Han, L.; An, N.; Xing, L.; Ma, H.; Cheng, L.; Yang, J.; Zhang, Q. Enhanced visible-light photocatalytic activity of carbonate-doped anatase TiO_2 based on the electron-withdrawing bidentate carboxylate linkage. *Appl. Catal. B Environ.* **2017**, *202*, 642–652. [CrossRef]
42. Chen, J.; Qiu, F.; Zhang, Y.; Liang, J.; Zhu, H.; Cao, S. Enhanced supercapacitor performances using C-doped porous TiO_2 electrodes. *Appl. Surf. Sci.* **2015**, *356*, 553–560. [CrossRef]
43. Payormhorm, J.; Idem, R. Synthesis of C-doped TiO_2 by sol-microwave method for photocatalytic conversion of glycerol to value-added chemicals under visible light. *Appl. Catal. A Gen.* **2020**, *590*, 117362. [CrossRef]
44. Cao, S.; Xue, Z.; Yang, C.; Qin, J.; Zhang, L.; Yu, P.; Wang, S.; Zhao, Y.; Zhang, X.; Liu, R. Insights into the Li+ storage mechanism of TiC@C-TiO2core-shell nanostructures as high performance anodes. *Nano Energy* **2018**, *50*, 25–34. [CrossRef]
45. Liu, G.; He, F.; Zhang, J.; Li, L.; Li, F.; Chen, L.; Huang, Y. Yolk-shell structured Fe_3O_4@C@F-TiO_2 microspheres with surface fluorinated as recyclable visible-light driven photocatalysts. *Appl. Catal. B Environ.* **2014**, *150-151*, 515–522. [CrossRef]
46. Qin, Y.; Zhuang, Y.; Lv, R.; Wang, T.; Wang, W.; Wang, C. Pd nanoparticles anchored on carbon-doped TiO_2 nanocoating support for ethanol electrooxidation in alkaline media. *Electrochim. Acta* **2015**, *154*, 77–82. [CrossRef]
47. Zhao, D.; Zhang, X.; Sui, L.; Wang, W.; Zhou, X.; Cheng, X.; Gao, S.; Xu, Y.; Huo, L. C-doped TiO_2 nanoparticles to detect alcohols with different carbon chains and their sensing mechanism analysis. *Sens. Actuat B Chem.* **2020**, *312*, 127942. [CrossRef]
48. Zou, Y.; Shi, J.; Ma, D.; Fan, Z.; Lu, L.; Niu, C. In situ synthesis of C-doped TiO_2@g-C_3N_4 core-shell hollow nanospheres with enhanced visible-light photocatalytic activity for H_2 evolution. *Chem. Eng. J* **2017**, *322*, 435–444. [CrossRef]
49. Yang, C.; Qin, J.; Xue, Z.; Ma, M.; Zhang, X.; Liu, R. Rational design of carbon-doped TiO_2 modified g-C_3N_4 via in-situ heat treatment for drastically improved photocatalytic hydrogen with excellent photostability. *Nano Energy* **2017**, *41*, 1–9. [CrossRef]
50. Dhanasekaran, P.; Selvaganesh, S.; Bhat, S.D. Nitrogen and carbon doped titanium oxide as an alternative and durable electrocatalyst support in polymer electrolyte fuel cells. *J. Power Sources* **2016**, *304*, 360–372. [CrossRef]

51. Han, X.; An, L.; Hu, Y.; Li, Y.; Hou, C.; Wang, H.; Zhang, Q. Ti_3-C_2 MXene-derived carbon-doped TiO_2 coupled with g-C_3N_4 as the visible-light photocatalysts for photocatalytic H_2 generation. *Appl. Catal. B Environ.* **2020**, *265*, 118539. [CrossRef]
52. Qin, Y.; Li, Y.; Lv, R.; Wang, T.; Wang, W.; Wang, C. Enhanced methanol oxidation activity and stability of Pt particles anchored on carbon-doped TiO_2 nanocoating support. *J. Power Sources* **2015**, *278*, 639–644. [CrossRef]
53. Aragaw, B.A.; Pan, C.; Su, W.; Chen, H.; Rick, J.; Hwang, B. Facile one-pot controlled synthesis of Sn and C codoped single crystal TiO_2 nanowire arrays for highly efficient photoelectrochemical water splitting. *Appl. Catal. B Environ.* **2015**, *163*, 478–486. [CrossRef]
54. Li, Y.; Shen, J.; Li, J.; Liu, S.; Yu, D.; Xu, R.; Fu, W.; Lv, X. Constructing a novel strategy for carbon-doped TiO_2 multiple-phase nanocomposites toward superior electrochemical performance for lithium ion batteries and the hydrogen evolution reaction. *J. Mater. Chem. A* **2017**, *5*, 7055–7063. [CrossRef]
55. Ivanov, S.; Barylyak, A.; Besaha, K.; Dimitrova, A.; Krischok, S.; Bund, A.; Bobitski, J. Enhanced lithium ion storage in TiO_2 nanoparticles, induced by sulphur and carbon co-doping. *J. Power Sources* **2016**, *326*, 270–278. [CrossRef]
56. Nouri, E.; Mohammadi, M.R.; Lianos, P. Impact of preparation method of TiO_2-RGO nanocomposite photoanodes on the performance of dye-sensitized solar cells. *Electrochim. Acta* **2016**, *219*, 38–48. [CrossRef]
57. Guan, D.; Yu, Q.; Xu, C.; Tang, C.; Zhou, L.; Zhao, D.; Mai, L. Aerosol synthesis of trivalent titanium doped titania/carbon composite microspheres with superior sodium storage performance. *Nano Res.* **2017**, *10*, 4351–4359. [CrossRef]
58. Zhang, Y.; Zhao, Y.; Cao, S.; Yin, Z.; Cheng, L.; Wu, L. Design and Synthesis of Hierarchical SiO_2@C/TiO_2 Hollow Spheres for High-Performance Supercapacitors. *ACS Appl. Mater. Interfaces* **2017**, *9*, 29982–29991. [CrossRef]
59. Zhang, Y.; Chen, J.; Tang, H.; Xiao, Y.; Qiu, S.; Li, S.; Cao, S. Hierarchically-structured SiO_2-Ag@TiO_2 hollow spheres with excellent photocatalytic activity and recyclability. *J. Hazard. Mater.* **2018**, *354*, 17–26. [CrossRef]
60. Yin, Z.; Qiu, S.; Chen, W.; Li, H.; Cheng, L.; Cao, S. Highly photocatalytic activity from tri-modified TiO_2 hollow spheres. *Mater. Let.* **2018**, *214*, 202–204. [CrossRef]
61. Varnagiris, S.; Medvids, A.; Lelis, M.; Milcius, D.; Antuzevics, A. Black carbon-doped TiO2 films: Synthesis, characterization and photocatalysis. *J. Photoch. Photobio. A* **2019**, *382*, 111941. [CrossRef]
62. Fittipaldi, M.; Gombac, V.; Montini, T.; Fornasiero, P.; Graziani, M. A high-frequency (95 GHz) electron paramagnetic resonance study of B-doped TiO_2photocatalysts. *Inorg. Chim. Acta* **2008**, *361*, 3980–3987. [CrossRef]
63. Liu, N.; Chen, X.; Zhang, J.; Schwank, J.W. A review on TiO_2-based nanotubes synthesized via hydrothermal method: Formation mechanism, structure modification, and photocatalytic applications. *Catal. Today* **2014**, *225*, 34–51. [CrossRef]
64. Murdoch, M.; Waterhouse, G.; Nadeem, M.; Metson, J.; Keane, M.; Howe, R.; Llorca, J.; Idriss, H. The effect of gold loading and particle size on photocatalytic hydrogen production from ethanol over Au/TiO_2 nanoparticles. *Nat. Chem.* **2011**, *3*, 489–492. [CrossRef] [PubMed]
65. Wu, N.; Wang, J.; Tafen, D.N.; Wang, H.; Zheng, J.; Lewis, J.P.; Liu, X.; Leonard, S.S. Shape-Enhanced Photocatalytic Activity of Single-Crystalline Anatase TiO_2 (101) Nanobelts. *J. Am. Chem. Soc.* **2010**, *132*, 6679–6685. [CrossRef] [PubMed]
66. Matos, J.; Riquelme, J.O.; Poon, P.S.; Montana, R.; Garcia, X.; Campos, K.; Garrido, J.C.H.; Titirici, M.M. C-doped anatase TiO_2: Adsorption kinetics and photocatalytic degradation of methylene blue and phenol, and correlations with DFT estimations. *J. Colloid Interface Sci.* **2019**, *547*, 14–29. [CrossRef]
67. Chen, J.; Qiu, F.; Xu, W.; Cao, S.; Zhu, H. Recent progress in enhancing photocatalytic efficiency of TiO_2-based materials. *Appl. Catal. A Gen.* **2015**, *495*, 131–140. [CrossRef]
68. Vimonses, V.; Jin, B.; Chow, C.W.K.; Saint, C. An adsorption-photocatalysis hybrid process using multi-functional-nanoporous materials for wastewater reclamation. *Water Res.* **2010**, *44*, 5385–5397. [CrossRef]
69. Lin, Y.; Weng, C.; Chen, F. Key operating parameters affecting photocatalytic activity of visible-light-induced C-doped TiO_2 catalyst for ethylene oxidation. *Chem. Eng. J.* **2014**, *248*, 175–183. [CrossRef]
70. Zhang, J.; Vasei, M.; Sang, Y.; Liu, H.; Claverie, J.P. TiO_2@carbon photocatalysts: The effect of carbon thickness on catalysis. *ACS Appl. Mater. Inter.* **2016**, *8*, 1903–1912. [CrossRef]

71. Liu, H.; Li, W.; Shen, D.; Zhao, D.; Wang, G. Graphitic carbon conformal, coating of mesoporous TiO_2 hollow spheres for high-performance lithium ion battery anodes. *J. Am. Chem. Soc.* **2015**, *137*, 13161–13166. [CrossRef] [PubMed]
72. Cheng, L.; Qiu, S.; Chen, J.; Shao, J.; Cao, S. A Practical Pathway for the preparation of Fe_2O_3 decorated TiO_2 photocatalyst with enhanced visible-light photoactivity. *Mater. Chem. Phys.* **2017**, *190*, 53–61. [CrossRef]
73. Marszewski, M.; Marszewska, J.; Pylypenko, S.; Jaroniec, M. Synthesis of Porous Crystalline Doped Titania Photocatalysts Using Modified Precursor Strategy. *Chem. Mater.* **2016**, *28*, 7878–7888. [CrossRef]
74. Yuan, Y.; Ruan, Z.; Huang, X.; Jiang, Y.; Tan, H. Energy-absorption-based explanation of the TiO_2/C photocatalytic activity enhancement mechanism. *J. Catal.* **2017**, *348*, 246–255. [CrossRef]
75. Wei, W.; Yu, C.; Zhao, Q.; Qian, X.; Li, G.; Wan, Y. Synergy effect in photodegradation of contaminants from water using ordered mesoporous carbon-based titania catalyst. *Appl. Catal. B Environ.* **2014**, *146*, 151–161. [CrossRef]
76. Zhao, X.; Zhang, Y.; Wu, M.; Szeto, W.; Wang, Y.; Pan, W.; Leung, D.Y.C. Carbon doped ultra-small TiO_2 coated on carbon cloth for efficient photocatalytic toluene degradation under visible LED light irradiation. *Appl. Surf. Sci.* **2020**, *527*, 146780. [CrossRef]
77. Mohamed, M.A.; Rahman, N.A.; Zain, M.F.M.; Minggu, L.J.; Kassim, M.B.; Jaafar, J.; Samad, S.; Mastuli, M.S.; Wong, R.J. Hematite microcube decorated TiO_2 nanorods as heterojunction photocatalyst with in-situ carbon doping derived from polysaccharides bio-templates hydrothermal carbonization. *J. Alloys Compd.* **2020**, *820*, 153143. [CrossRef]
78. Noorimotlagh, Z.; Kazeminezhad, I.; Jaafarzadeh, N.; Ramezani, Z. Improved performance of immobilized TiO_2 under visible light for the commercial surfactant degradation: Role of carbon doped TiO_2 and anatase/rutile ratio. *Catal. Today* **2020**, *348*, 277–289. [CrossRef]
79. Maria, C.A.T.; Chiu, J.F.V.; López, J.M.H.; Rosa, J.R.; Barbieri, V.; Siligardi, C.; González, E.I.C. Microplastic pollution reduction by a carbon and nitrogen-doped TiO_2: Effect of pH and temperature in the photocatalytic degradation process. *J. Hazard. Mater.* **2020**, *395*, 122632.
80. Zhao, Y.; Li, X.; Tian, C.; Wang, J. Production of carbon-doped titanium dioxide (C-TiO_2) from polytitanium-coagulated sludge as an adsorbent or photocatalyst for pollutant removals. *J. Clean Prod.* **2020**, *267*, 121979. [CrossRef]
81. Wang, Y.; Chen, Y.; Barakat, T.; Wang, T.; Krief, A.; Zeng, Y.; Laboureur, M.; Fusaro, L.; Liao, H.; Su, B. Synergistic effects of carbon doping and coating of TiO_2 with exceptional photocurrent enhancement for high performance H_2 production from water splitting. *J. Energy Chem.* **2021**, *56*, 141–151. [CrossRef]
82. Venditti, F.; Cuomo, F.; Ceglie, A.; Avino, P.; Russo, M.V.; Lopez, F. Visible Light Caffeic Acid Degradation by Carbon-Doped Titanium Dioxide. *Langmuir* **2015**, *31*, 3627–3634. [CrossRef] [PubMed]
83. Huang, X.; Yang, W.; Zhang, G.; Yan, L.; Zhang, Y.; Jiang, A.; Xu, H.; Zhou, M.; Liu, Z.; Tang, H.; et al. Alternative synthesis of nitrogen and carbon co-doped TiO_2 for removing fluoroquinolone antibiotics in water under visible light. *Catal. Today* **2020**. [CrossRef]
84. El-Sheikh, S.M.; Zhang, G.; El-Hosainy, H.M.; Ismail, A.A.; O'Shea, K.E.; Falaras, P.; Kontos, A.G.; Dionysiou, D.D. High performance sulfur, nitrogen and carbon doped mesoporous anatase-brookite TiO_2 photocatalyst for the removal of microcystin-LR under visible light irradiation. *J. Hazard. Mater.* **2014**, *280*, 723–733. [CrossRef] [PubMed]
85. Shayegan, Z.; Haghighat, F.; Lee, C. Carbon-doped TiO_2 film to enhance visible and UV light photocatalytic degradation of indoor environment volatile organic compounds. *J. Environ. Chem. Eng.* **2020**, *8*, 104162. [CrossRef]
86. Shen, Z.; Wang, G.; Tian, H.; Sunarso, J.; Liu, L.; Liu, J.; Liu, S. Bi-layer photoanode films of hierarchical carbon-doped brookite-rutile TiO_2 composite and anatase TiO_2 beads for efficient dye-sensitized solar cells. *Electrochim. Acta* **2016**, *216*, 429–437. [CrossRef]
87. Elmouwahidi, A.; Garcıa, E.B.; Quiben, J.C.; Cadenas, A.F.P.; Maldonado-Hodar, F.J.; Carrasco-Marın, F. Carbon-TiO_2 composites as high-performance supercapacitor electrodes: Synergistic effect between carbon and metal oxide phases. *J. Mater. Chem. A* **2018**, *6*, 633–644. [CrossRef]
88. Zhu, H.; Jing, Y.; Pal, M.; Liu, Y.; Liu, Y.; Wang, J.; Zhang, F.; Zhao, D. Mesoporous TiO_2@N-doped Carbon Composite Nanospheres Synthesized by Direct Carbonization of Surfactants after Sol-gel Process for Superior Lithium Storage. *Nanoscale* **2017**, *9*, 1539–1546. [CrossRef]

89. Geng, H.; Ming, H.; Ge, D.; Zheng, J.; Gu, H. Designed fabrication of fluorine-doped carbon coated mesoporous TiO_2 hollow spheres for improved lithium storage. *Electrochim. Acta* **2015**, *157*, 1–7. [CrossRef]
90. Zhu, Q.; Xie, C.; Li, H.; Yang, C.; Zeng, D. A novel planar integration ofall-solid-state capacitor and photodetector by an ultra-thin transparentsulfated TiO_2 film. *Nano Energy* **2014**, *9*, 252–263. [CrossRef]
91. Yin, Z.; Shao, J.; Tang, W.; Sheng, W.; Sun, D.; Xiao, Y.; Cao, S. Design and synthesis of 'single-crystal-like' C-doped TiO_2 nanorods for high-performance supercapacitors. *Nanotechnology* **2020**, *31*, 275401. [CrossRef] [PubMed]
92. Li, B.; Zhao, W.; Yang, Z.; Zhang, C.; Dang, F.; Liu, Y.; Jin, F.; Chen, X. A carbon-doped anatase TiO_2-Based flexible silicon anode with high-performance and stability for flexible lithium-ion battery. *J. Power Sources* **2020**, *466*, 228339. [CrossRef]
93. Goriparti, S.; Miele, E.; Prato, M.; Scarpellini, A.; Marras, S.; Monaco, S.; Toma, A.; Messina, G.C.; Alabastri, A.; Angelis, F.D.; et al. Direct Synthesis of Carbon-Doped TiO_2-Bronze Nanowires as Anode Materials for High Performance Lithium-Ion Batteries. *ACS Appl. Mater. Inter.* **2015**, *7*, 25139–25146. [CrossRef] [PubMed]
94. Chen, J.; Qiu, F.; Zhang, Y.; Cao, S. Carbon-Doped Hollow Titania with Tuneable Shell Architecture for Supercapacitors. *Aust. J. Chem.* **2016**, *69*, 183–190. [CrossRef]
95. Xiao, Y.; Sun, X.; Li, L.; Chen, J.; Zhao, S.; Jiang, C.; Yang, L.; Cheng, L.; Cao, S. Simultaneous formation of a C/N-TiO_2 hollow photocatalyst with efficient photocatalytic performance and recyclability. *Chin. J. Catal.* **2019**, *40*, 765–775. [CrossRef]
96. Hua, Z.; Dai, Z.; Bai, X.; Ye, Z.; Gu, H.; Huang, X. A facile one-step electrochemical strategy of doping iron, nitrogen, and fluorine into titania nanotube arrays with enhanced visible light photoactivity. *J. Hazard. Mater.* **2015**, *293*, 112–121. [CrossRef]
97. Tang, W.; Chen, J.; Yin, Z.; Sheng, W.; Lin, F.; Xu, H.; Cao, S. The complete removal of phenolic contaminants from bismuth-modified TiO_2 single crystal photocatalyst. *Chin. J. Catal.* **2021**, *42*, 347–355. [CrossRef]

Publisher's Note: MDPI stays neutral with regard to jurisdictional claims in published maps and institutional affiliations.

© 2020 by the authors. Licensee MDPI, Basel, Switzerland. This article is an open access article distributed under the terms and conditions of the Creative Commons Attribution (CC BY) license (http://creativecommons.org/licenses/by/4.0/).